Normative Modeling Using Multimodal Variational Autoencoders to Identify Individual Heterogeneity in Alzheimer's Disease

Sayantan Kumar[1,3], Thomas Earnest[2], Philip R.O. Payne[1,3], Aristeidis Sotiras[3,4] for the Alzheimer's Disease Neuroimaging Initiative*

Abstract

Background and Objectives

Alzheimer's disease (AD) is highly heterogenous, with significant variations in both clinical presentation and neurobiology. To explore this, we used normative modelling on multimodal neuroimaging data to index spatial patterns of neuroanatomical and neuropathological variability in AD participants. Furthermore, we quantify group differences in between-participant dissimilarity for each modality. Finally, we proposed a disease severity index based on outlier deviations, assessed the relationships between the severity index and cognitive function and examined whether the disease index was predictive of disease progression.

Methods

Multimodal regional brain data were obtained in the form of gray matter volumes from T1-weighted MRI scans, amyloid SUVR (Standardized Uptake Value Ratio) from Florbetapir ^{18}F AV45 amyloid PET and tau SUVR from Florbetapir ^{18}F AV1451 tau PET scans respectively. A multimodal variational autoencoder-based normative model, adjusted on age and sex, was trained on cognitively unimpaired subjects (Clinical Dementia Rating [CDR®] = 0 and without amyloid positivity). The trained model was subsequently used to estimate regional Z-scores brain map for each individual with AD, measuring the deviation from the norm for each modality. Finally, statistical outliers were identified and a disease severity index was calculated for each AD participant.

Results

Subjects in the advanced AD stages (a) have more morphological and pathological brain changes, (b) have more within-group heterogeneity and (c) have a higher proportion of outlier regional deviations than people with preclinical AD and healthy controls. It was also

observed that subject-level heterogeneity in MRI atrophy (neuroanatomical heterogeneity) and amyloid and tau deposition (neuropathological heterogeneity) are (a) significantly associated with cognitive performance and (b) can be potential markers to predict survival time before AD progression to advanced CDR stages.

Discussion

Individualized normative maps of brain atrophy, amyloid and tau loading highlight the heterogeneous effect of AD on the brain. The disease severity index based on regional outlier estimates can be potentially used to track an individual's disease progression or treatment response in clinical trials.

Author affiliation:

[1]Department of Computer Science and Engineering, Washington University in St. Louis, St. Louis, Missouri, USA
[2]Division of Computational and Data Sciences, Washington University in St. Louis, St. Louis, Missouri, USA
[3]Institute for Informatics, Washington University School of Medicine, St. Louis, Missouri, USA
[4]Department of Radiology, Washington University in School of Medicine, St. Louis, Missouri, USA

*Data used in the preparation of this article were obtained from the Alzheimer's Disease Neuroimaging Initiative (ADNI) database (adni.loni.usc.edu). As such, the investigators within the ADNI contributed to the design and implementation of ADNI and/or provided data but did not participate in the analysis or writing of this report. A complete listing of ADNI investigators can be found at:
http://adni.loni.usc.edu/wpcontent/uploads/how_to_apply/ADNI_Acknowledgement_List.pdf

Correspondence to: Aristeidis Sotiras
Full address: Department of Radiology, Washington University in School of Medicine, St. Louis, Missouri, USA
E-mail: aristeidis.sotiras@wustl.edu

Keywords: Normative modelling; ADNI; Alzheimer Disease; heterogeneity; ATN; multimodal variational autoencoders

Abbreviations/Glossary: ADNI = Alzheimer's Disease Neuroimaging Initiative; AD = Alzheimer's disease; HC = healthy controls; CDR = Clinical Dementia Rating; FDR = False Discovery Rate; UKB = UK Biobank; IQR = Interquartile range; SUVR = Standardized Uptake Value Ratio

Introduction

Alzheimer disease (AD) is the most common cause of dementia, which is a syndrome of impaired memory and/or thinking that interferes with activities of daily life.[1,2] AD-related brain pathology, which begins almost 10-20 years before the onset of dementia symptoms, is associated with the accumulation and deposition of amyloid-β peptide and tau protein leading to neurodegeneration.[3] AD is highly heterogeneous, with significant variations in clinical presentations, cognitive impairments, disease progression rates, and underlying neuropathological changes of individual subjects.[4] Conventional statistical analyses in AD research primarily focus on group averages, assuming that the disease affects all subjects in similar ways, characterizing the average subject. These approaches overlook the inherent heterogeneity between individuals and fail to account for each subject's unique characteristics.[5] To advance toward the goal of precision medicine in AD, it is imperative to move beyond the average and design approaches that reflect heterogeneity at the individual subject level.

Large neuroimaging datasets like Alzheimer's Disease Neuroimaging Initiative (ADNI), Open Access Series of Imaging Studies (OASIS) and UKB (UK Biobank) have supported the development and application of data-driven methods for analyzing heterogeneity in AD research[6,7]. These datasets integrate information from multiple neuroimaging modalities: (a) structural magnetic resonance imaging (MRI), which can be used to measure both the neuroanatomical changes in the brain (atrophy) and (b) positron emission tomography (PET), which can measure the pathophysiological changes (amyloid and tau deposition in the brain). Each modality provides unique and complementary information about the disease, allowing for a more comprehensive understanding of AD pathology, progression, and individual differences.[8] This multimodal approach has the potential to improve diagnostic accuracy, enhance predictive models, identify subtypes or clusters of subjects with distinct disease profiles, and guide personalized treatment strategies. [9,10]

Multimodal neuroimaging datasets have enabled the estimation of biological subtypes of AD, as a way to disentangle heterogeneity by grouping subjects based on distinctive neurobiological and cognitive characteristics.[7,11–14] However, there are challenges associated with the clinical translation of neuroimaging-derived subtypes. These include the clinical

validity of the subtypes and how stable subtypes are over the disease course.[7,13,15] Further, clustering assumes homogeneity of subjects within each cluster, limiting the extent of individual-level heterogeneity in the sample.[16] Gaining insights into the neurobiology of Alzheimer's disease (AD) at the individual subject level can offer a detailed comprehension of their condition and enable customized treatment approaches.[17] Nonetheless, despite the well-established concept of subject-centered, individualized precision medicine for AD, current research endeavors remain constrained in scope and magnitude.

Normative modelling can parse heterogeneity in neurodegenerative and neuropsychiatric clinical cohorts while allowing predictions at an individual subject level.[18] It assumes that disorders in individual subjects manifest as deviations from a normal pattern of functioning, quantifying how each subject deviates from the expected normative pattern learned in a distribution of cognitively unimpaired (CU) subjects.[19–25] The procedure of normative modelling in the context of AD is a two-fold approach: (i) machine learning models are estimated using data from a reference cohort of cognitively unimpaired participants and (ii) the estimated model is applied to a target clinical cohort of AD subjects.[26] A diseased individual can then be located within the normative distribution to establish to what extent they deviate from the expected pattern in each measure, and a map can be generated of where and to what extent an individual's brain differs from the norm.[21,22] Previous studies have used only single modality neuroimaging data (e.g. structural MRI) to analyse AD heterogeneity by normative modelling.[25–27] However, these studies do not take into account the interaction between multiple modalities (e.g. MRI and PET), which is essential for understanding the biology of a multifactorial disease like AD.[28]

The diversity observed among individual subjects (subject-level heterogeneity) may result from the differential distribution and severity of neuroanatomical/pathological changes in various brain regions (spatial heterogeneity). In this study, we examined both subject-level and spatial heterogeneity in AD subjects using multimodal normative modelling. We applied our previous implementation of multimodal variational autoencoders and used it to model the joint distribution between multiple neuroimaging modalities (e.g. MRI and PET).[28] Our proposed multimodal normative modelling framework takes regional grey matter volumes, amyloid and tau signals as the 3 modalities, combines important modality-specific information in a joint latent space and learns the neuroanatomical (grey matter volumes) and pathophysiological (amyloid, tau) characteristics of the healthy brain. Further, our model

estimates how subjects with different stages of AD deviate with respect to cognitively unimpaired subjects and identifies the statistical outliers. We propose a new disease severity index for each patient which captures both the spatial extent of outliers and the magnitude of regional outlier deviations, quantifying the spatial patterns of heterogeneity using the modality-specific regional deviations. Specifically, we aimed to (a) assess the spatial (regional) patterns of neuroanatomical and neuropathological variability in AD participants based on overlapping or distinct pattern of outlier deviations, (b) quantify group differences in between-participant dissimilarity (patient-level heterogeneity) for each modality, (c) estimate the correlation between modality-specific disease severity and cognitive performance and (d) finally examine whether the disease severity index relates to subsequent disease progression. Our choice of experiments (visualizations) are similar in idea to Verdi et. al [25] which used cortical thickness measures from MRI to measure neuroanatomical heterogeneity in AD. To the best of our knowledge, ours is the first study that explores AD heterogeneity across multiple neuroimaging modalities (MRI and PET), through the lens of individualized subject variations.

Materials and Methods

Participants

The study included participants from two distinct datasets: (a) a reference control dataset consisting of cognitively unimpaired individuals spanning various age groups, and (b) a disease target dataset of AD subjects. Subjects with no cognitive impairment (Clinical Dementia Rating [CDR®] = 0) and without amyloid pathology were selected from the Knight ADRC (Alzheimer's Disease Research Center) at Washington University in St Louis and the Alzheimer's Disease Neuroimaging Initiative (ADNI3) dataset.[29] Subjects with amyloid positivity (AD continuum)were selected from the ADNI and the Knight ADRC dataset respectively. The criteria for study inclusion for both the control and clinical datasets were the simultaneous availability of baseline scans of T1-weighted MRI, amyloid PET and tau PET respectively, all of which should be dated within 1 year of one another. Participants with any of the 3 modalities missing were excluded from our study. AD subjects in the target disease set were stratified into the following categories in increasing order of disease severity (a) preclinical stage with no symptoms (CDR = 0, A+), (b) CDR = 0.5 and (c) CDR >= 1.

Harmonization between ADNI and Knight ADRC

Combining imaging data from multiple sites and studies is challenging due to a lack of standardization in image acquisition protocols, scanner hardware and software. To ensure data harmonization between ADNI and Knight ADRC, the COMBAT-GAM harmonization strategy was applied to correct multi-site data.[30] COMBAT-GAM implemented the COMBAT algorithm[31] with Generalized Additive Models (GAM) to account for the non-linear effects of covariates age and sex. The harmonization algorithm was trained on the healthy controls across both ADNI and Knight ADRC and the pre-trained model was applied to the disease dataset across both the sources. The one-way ANOVA method was used to estimate if the regional differences between ADNI and KARI are significant for each of the 3 modalities, both before and after harmonization. The regional p-value maps were visualized through the ggseg package in python.

Standard Protocol Approvals. Registrations and Subject Consent

Written informed consent was obtained from all ADNI participants before experimental procedures were performed. Approval was received by an ethical standards committee for ADNI study data use. All Knight ADRC participants signed a standard informed consent document, and all procedures were approved by the Institutional Review Board at Washington University in St. Louis.

MRI Acquisition and Processing

From both ADNI3 and Knight ADRC databases, T1-weighted MRI images were acquired using 3T MRI scanners. Detailed MRI protocols for T1-weighted sequences in ADNI are available online. (https://adni.loni.usc.edu/methods/documents/mri-protocols/)[32] MRI data for Knight ADRC were acquired on a Siemens Biograph mMR or Trio 3T scanner. The T1-weighted MRI sequences from both the data sources underwent volumetric segmentation with Freesurfer version 5.3 (Knight ADRC) or Freesurfer version 6 (ADNI3). The Freesurfer estimation was performed using the “recon-all” command (see [33] for more information). From T1- weighted MRI scans, the cortical surface of each hemisphere was parcellated according to the Desikan–Killiany atlas[34] and anatomical volumetric measures were obtained via a whole-brain segmentation procedure (Aseg atlas).[35] The final data included regional grey matter volumes of 66 cortical regions and 24 subcortical regions for each participant. All regional volumes were normalized by their intracranial volume (ICV).

PET Acquisition and Processing

Amyloid PET imaging and tau PET imaging for both ADNI and Knight ADRC were collected with Florbetapir ^{18}F AV45 and Flortaucipir ^{18}F AV1451 as the radiotracer respectively and converted to standardized uptake value ratios (SUVRs), with the cerebellar cortex serving as the reference region. Amyloid positive (A+) and amyloid negative (A-) groups were determined by applying a cut-off of 1.11 for the global Florbetapir SUVR (Standardized Uptake Value Ratio) in the ADNI dataset[36] and a cut-off of 1.24 for mean cortical SUVR in the Knight ADRC database.[37] Similar to MRI, amyloid and tau SUVR were calculated for the same set of 66 cortical and 24 subcortical regions. For the Knight ADRC dataset, PET data were processed using an in-house pipeline that utilized regions of interest derived from FreeSurfer, known as the PET Unified Pipeline (github.com/ysu001/PUP).

Multimodal Normative Modeling

Joint distribution between multiple modalities

Our proposed multimodal normative modelling framework is a multimodal variational autoencoder (VAE) with separate modality-specific encoders and decoders for individual modalities.[28] Each modality data was passed through a modality-specific encoder to obtain the corresponding latent space parameters (mean and variance). The mean and variance of the 3 modalities were combined by the Product-of-Experts (PoE)[38,39] approach to obtain a unified shared latent space in which important information was combined from all 3 modalities. The shared latent parameters are then passed through modality-specific decoders to obtain the corresponding reconstructions. The main idea is to assume that the joint distribution over the multiple modalities factorizes into a product of single-modality data-generating distributions when conditioned on the latent space. The shared latent space models the joint distribution between the multiple modalities. For detailed mathematical derivation, see Supplementary material.

Conditioning VAE on covariates

We conditioned the multimodal VAE on the age and sex of participants, to ensure that the modality-specific deviations reflect only disease pathology and not deviations due to the effects of covariates. Both age and sex were transformed into one-hot encoding vectors. After this transformation, each subject had an age vector with 44 positions, where each position

corresponds to a year within the range of 47–91 years. The modality-specific decoders used these vectors and the latent code to reconstruct the brain data.

Model training and testing

Regional grey matter volumes (T1-weighted MRI), amyloid SUVR (AV45 PET) and tau SUVR (AV1451 PET) were used as the multimodal input for the multimodal VAE. The model was first trained on multimodal data of healthy controls and learns to reconstruct the input as closely as possible to the original. The trained model is then applied to subjects in the target disease dataset to assess the model sensitivity in estimating the extent to which AD subjects deviate from the normal trend. The main idea of the normative approach is that since the multimodal VAE only learns how to reconstruct data of healthy controls, the reconstructions will be less precise (more reconstruction error) for AD subjects. The deviations for each modality of disease subjects can be calculated independently as the squared difference between input and reconstructed data. To account for the fact that the model may not be able to perfectly reconstruct the data of healthy subjects, the deviations were normalized with respect to the deviations (mean and variance) of healthy controls obtained from a separate holdout validation cohort. This process generated regional modality-specific Z-scores for each subject in the disease dataset, relative to the normative range of healthy controls. Note that the Z-scores are already adjusted on the age and sex of subjects due to the conditional nature of our multimodal VAE.

Statistical Analysis

We identified the brain regions of each subject whose modality-specific normalized deviations (Z-scores) were significantly different from those of the healthy controls ($p < 0.05$). Since the Z-scores were estimated independently for each brain region for every subject, FDR (False Discovery Rate) correction was applied to control the Type 1 error rate. [40] For MRI grey matter volumes, regions with $Z < -1.96$ ($p < 0.05$ after FDR correction) corresponded to the bottom 2.5% of the normative distribution and were marked as outliers (anomalies). Similarly, for amyloid and tau, $Z > +1.96$ (FDR-corrected $p < 0.05$) were labelled as outliers (anomalies), corresponding to the top 2.5% of the normative distribution. We only used a lower bound threshold for MRI outliers and an upper bound threshold for amyloid and tau outliers, since we are interested in MRI atrophy (loss in grey matter volume) and amyloid/tau deposition (increase in SUVR). We propose a new disease severity index for

each subject, capturing both the spatial extent of outliers and the magnitude of regional outlier deviations. This new subject-level severity index was calculated by a dot product between the binary-thresholded outlier vector and the subject deviation (Z-scores) vector. Since different subjects have different number of outlier regions, the severity values of each subject were divided by the total number of regions across the 3 modalities (270 regions, 90 for each modality). The following experiments assessed both subject-level heterogeneity and spatial heterogeneity in MRI atrophy (neuroanatomical heterogeneity) and amyloid and tau loading (pathophysiological heterogeneity).

Sensitivity towards disease staging: Both the subject-level and the regional disease severity index were assessed for their sensitivity to AD staging groups to validate higher magnitude across progressive stages: healthy controls, preclinical (CDR = 0 A+), CDR = 0.5, CDR >= 1. Additionally, pairwise group comparisons in outlier deviations for each region (total of 90 regions - FDR corrected) were visualized using Cohen's f-statistic effect size maps (FDR corrected[40]) for each modality, adjusted for age and sex. High effect size corresponding to a region indicates significantly more grey matter volume atrophy (neurodegeneration) or amyloid/tau deposition (pathological abnormalities) in the brain compared to cognitively unimpaired subjects. The effect size brain maps were visualized through the ggseg package in Python.

Dissimilarity between subjects across modalities: The Hamming distance, a quantitative measure of similarity between binary thresholded FDR-corrected outlier vectors, was used to measure dissimilarity between individuals across all modalities. The dissimilarity maps, computed both across all modalities and for individual modalities, quantifies the heterogeneity of subjects within the same clinical group. Outlier distance density or the spread of outlier dissimilarity was also compared between the 4 staging groups to estimate the extent subjects within the different disease group differ from individuals with the same staging.

Proportion of outliers for each region: To explore spatial patterns of outliers per group for grey matter atrophy, amyloid and tau loading, we calculated the outlier frequency of each region. This is estimated by the proportion of participants within each group whose deviation was an outlier (i.e., FDR corrected $p < 0.05$). This enabled visualization of the extent to

which patterns of outlier regions overlap or are distinct. The outlier frequency brain atlas maps were mapped using the ggseg package in Python.

Associations with cognitive function: We estimated the association between the subject-level severity scores and cognitive composite scores from ADNI (memory using ADNI MEM[41] and executive function using ADNI EF[42]). ADNI-MEM is a composite memory score from the neuropsychological battery used in the ADNI dataset, derived from Rey Auditory Verbal Learning Test (RAVLT), AD Assessment Schedule-Cog (ADAS13-Cog), Mini-Mental State Exam (MMSE) and Logical Memory. ADNI-EF is a composite score measuring abilities broadly related to executive function (EF), including WAIS-R Digit Symbol Substitution, Digit Span Backwards, Trails A and B, Category Fluency, and Clock Drawing. For both ADNI-MEM and ADNI-EF, low scores indicate worse cognition performance. Age and sex-adjusted linear regressions were fitted between the severity values and cognition scores, with Pearson Correlation Coefficient measuring the correlation between them.

CDR Progression Analysis: We obtained follow-up CDR information from 316 subjects from both ADNI and Knight ADRC with CDR scores up to 7 years from baseline scan. 64 people with CDR < 1 at baseline had converted to CDR >= 1 within three years. Survival analysis using Cox proportional hazards regression model was performed to assess whether the subject-level disease severity values related to the risk of CDR progression, controlling for age and sex. We used a Kaplan–Meier plot to illustrate how the 4 quantiles of the severity scores can contribute to the risk of disease progression.

Data Availability

All Knight ADRC data reported in this manuscript are available to qualified parties from the corresponding author upon request. ADNI data used in this study are publicly available and can be requested following ADNI Data Sharing and Publications Committee guidelines: adni.loni.usc.edu/data-samples/access-data/. The implementation code for this study will be made available upon acceptance.

Results

Participants

Cognitively unimpaired subjects were selected from the ADNI (n = 434) and the Knight ADRC database (n = 301) respectively. 231 amyloid positive subjects from ADNI and 129 amyloid positive subjects from Knight ADRC were included as part of the target disease set (Table 1). The training set with harmonized data from ADNI and Knight ADRC was divided into 65% for model training and validation, and 15% holdout for estimating the mean and variance for normalizing the deviations of disease subjects. The remaining 20% of cognitively unimpaired (controls) plus amyloid-positive subjects were used to assess the neuroanatomical and pathophysiological presentation heterogeneity.

The COMBAT-GAM harmonization results show that the cognitively unimpaired subjects from both ADNI and Knight ADRC are well harmonized with very little regional differences for all the 3 modalities (eFigure 1). However, there still existed significant differences between the 2 datasets for the target disease set even after harmonization. The following sections show the heterogeneity results (subject-level and spatial) for the ADNI dataset. Corresponding results for the Knight ADRC dataset are presented in the Supplementary material.

Table 1: Demographics of disease subjects from ADNI and Knight ADRC

	ADNI	**Knight ADRC**	**p-value**
N (%)	231 (64%)	129 (36%)	-
Sex, Male: Female	108:123	48:81	$p = 7.5 \times 10^{-5}$
Age (mean +/- SD)	73.6 +/- 6.9	71.5 +/- 8.3	P = 0.03
CDR (0/0.5/>=1)	121/80/30	98/24/7	-
MMSE* (mean +/- SD)	23.5 +/ 3.2	26.5 +/ 3.7	$p = 3.6 \times 10^{-7}$
Amyloid centiloid (mean)	68	53.5	$p = 4.5 \times 10^{-12}$

Abbreviations: ADNI = Alzheimer's Disease Neuroimaging Initiative; ANOVA = analysis of variance; MMSE = Mini-Mental State Examination

Statistical differences were assessed using ANOVA (continuous) and chi-squared tests (categorical)

***** MMSE had a maximum score of 30

Subjects in the advanced AD stages have more morphological and neuropathological brain changes than people with preclinical AD and cognitively unimpaired subjects.

The subject-level severity scores (Z-scores) reflect the neuroanatomical alterations in the brain due to MRI atrophy and pathological changes in the brain due to amyloid and tau deposition, compared to the cognitively unimpaired subjects (Figure 1 A-D). The severity

scores for ADNI subjects show a monotonous increasing pattern across the AD stages and differed between groups overall for each of the 3 modalities: MRI ($p = 2 * 10^{-16}$), amyloid ($p = 3 * 10^{-15}$) and tau ($p = 7 * 10^{-15}$). Pairwise comparisons (Tukey post-hoc) across all modalities were all significant ($p < 0.05$) except between CU and preclinical for MRI and tau and between CDR = 0.5 and CDR >= 1 for amyloid. Severity scores across all modalities (Figure 1 bottom right) are the lowest in cognitively unimpaired subjects (mean = 0.06, IQR = 0.03, 95% CI = [0.007-0.1]), highest in CDR >= 1 (mean = 1.6, IQR = 1.5, 95% CI = [1.11-1.96]), and intermediate in preclinical (mean = 0.45, IQR = 0.6, 95% CI = [0.39-0.52]), CDR = 0.5 (mean = 1.1, IQR = 1.3, 95% CI = [0.87-1.25]) (Figure 1D). Results corresponding to the severity scores of Knight ADRC participants are presented in the Supplementary material (eFigure 2).

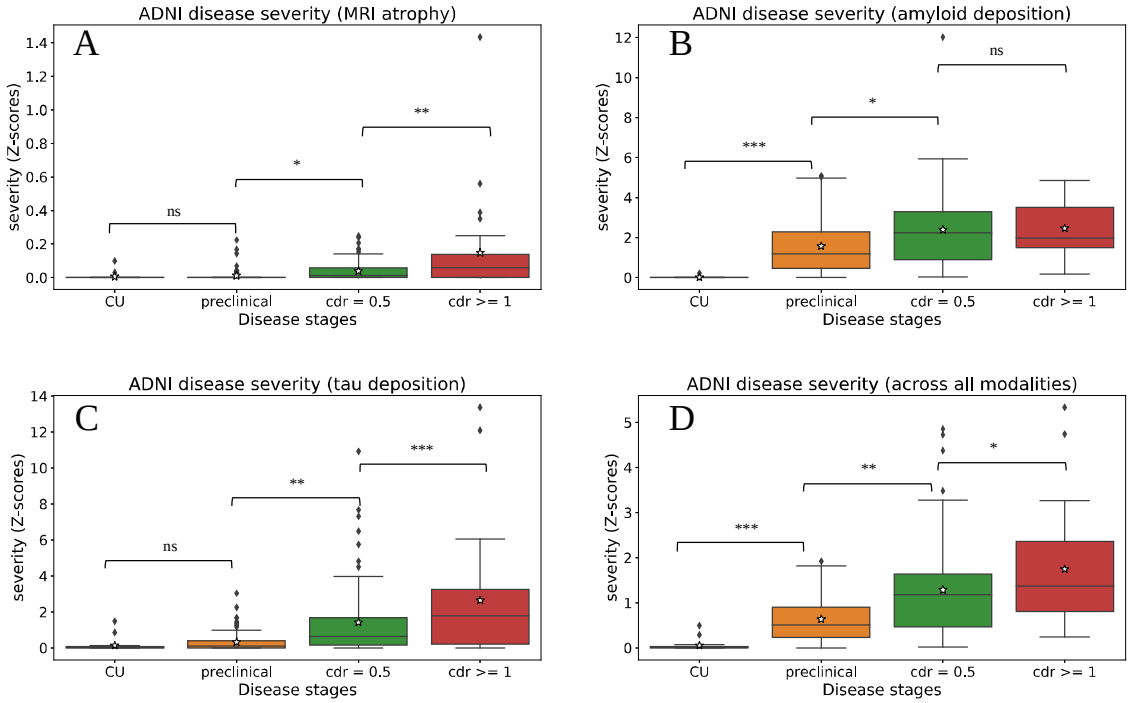

Figure 1: Box plot showing the disease severity scores (Z-scores) of ADNI participants across cognitively unimpaired subjects and the AD groups (in order of severity). The 4 subplots represent MRI, amyloid, tau and all modalities respectively in clockwise order. Pairwise comparisons (Tukey post-hoc) across all modalities were all significant ($p < 0.05$) except between CU and preclinical for MRI and tau and between CDR = 0.5 and CDR >= 1 for amyloid. **Abbreviations**: MRI: Magnetic Resonance Imaging, CU: Cognitively unimpaired, ADNI: Alzheimer's Disease Neuroimaging Initiative. **Statistical annotations**: ns: not significant $0.05 < p <= 1$, * $0.01 < p <= 0.05$, ** $0.001 < p < 0.01$, *** $p < 0.001$.

Region-level pairwise group comparisons in outlier deviations of ADNI participants show progressively higher effect size across disease stages when compared to cognitively unimpaired subjects for all 3 modalities (Figure 2). In general, effect sizes increase over progressive AD stages with subjects showing greater effect sizes for amyloid compared to tau and MRI. Preclinical AD subjects show no effect size for MRI and tau but for amyloid since preclinical AD was defined based on amyloid positive. The effect size maps show regional (spatial) heterogeneity both within and across modalities. Region-level group differences for MRI atrophy were most evident within the frontal, temporal and hippocampal and amygdala regions with maximum effect size in the amygdala and hippocampal regions. For amyloid, the differences to extend to all cortical regions, ventricles, and the amygdala with the accumbens area region showing the maximum effect size. Tau differences are most evident in the temporal, parietal, amygdala and ventricle regions with maximum effect size in the amygdala regions. The effect size maps of the Knight ADRC participants are presented in the Supplementary material (eFigure 3).

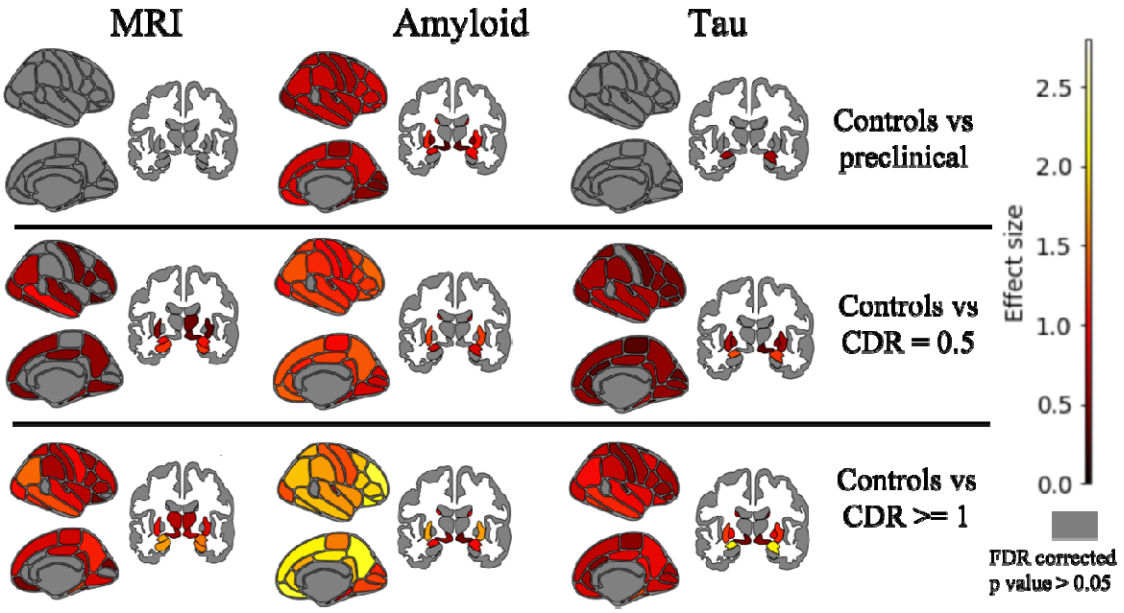

Figure 2: Brain atlas maps showing the region-level pairwise group differences (effect size maps) in deviations (ADNI) between cognitively unimpaired subjects and each of the AD stages for the 3 modalities: MRI, amyloid and tau respectively (left to right) The color bar represents the effect size (Cohen's d statistic) (0.5 is considered a small effect, 1.5 a medium effect and 2.5 large effect). Gray regions represent that no participants have statistically significant deviations after False Discovery Rate (FDR) correction.

Subjects in the advanced AD stages have more within-group heterogeneity than people with preclinical AD and cognitively unimpaired subjects.

Hamming distance matrices (calculated across all modalities) indicated greater within-group dissimilarity in ADNI subjects in the later stages of AD, relative to preclinical AD or cognitively unimpaired subjects, who were most similar to each other in spatial patterns of outlier deviations (Figure 3). The median hamming distance significantly differed between groups overall ($p = 5.6 * 10^{-25}$). Pairwise comparisons (Tukey post-hoc) were all significant ($p < 0.001$), with within-group dissimilarity higher in the CDR = 0.5 (median 76, IQR 42, 95% CI 77.6–78.7) and CDR>=1 group (median 82, IQR 43, 95% CI 82.4–85.7) and lowest in healthy controls (median 15, IQR 10, 95% CI 18.8–19.8) with preclinical AD being intermediate (median 59, IQR 42, 95% CI 60.8–61.4). Across all modalities, the high density of dissimilarity (Figure 3D) shows that the later stages of AD have more heterogeneity or inter-subject variability compared to the earlier stages (preclinical and healthy controls). If modality-specific outliers are considered, there exists more subject-level heterogeneity for tau compared to amyloid and MRI. The hamming distance matrices and the outlier density maps of the Knight ADRC participants are presented in the Supplementary material (eFigure 4).

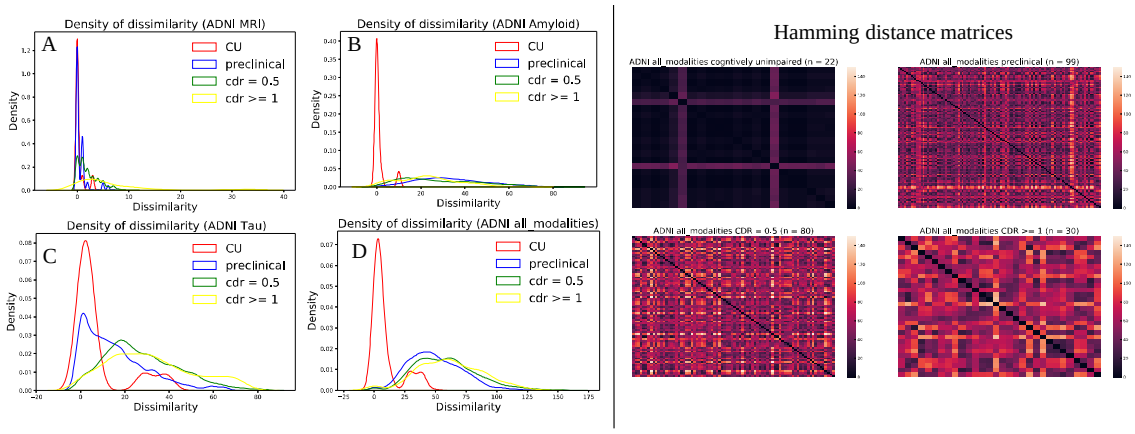

Figure 3: (**right**) Outlier distance heatmaps (Hamming distance between binary thresholded FDR-corrected outlier vectors across all modalities) for ADNI participants. Both x and y axis represent participants within each disease group. The numbers in parentheses in the figure titles indicate the number of participants within each group. Yellow indicates a higher Hamming distance (greater dissimilarity between participants in this brain region), as opposed to if participants are identical in this brain region, the Hamming distance would be 0, represented by white in the color bar. (**left**) Outlier distance density (kde plot): illustrates the spread of outlier dissimilarity (calculated by the Hamming distance) within each AD group. (A)-(D) represent the outlier distance density plots for MRI, amyloid, tau and across all modalities respectively.

Subjects in the advanced AD stages have a higher proportion of outlier subjects in neurodegeneration and pathological abnormalities

The proportion of outliers defined within each group (ADNI dataset) differed in regional patterns between CDR>=1, CDR = 0.5, preclinical and control groups (Figure 4). A high outlier proportion corresponding to a region indicates that the region has a higher number of subjects with outlier deviations than cognitively unimpaired subjects. In general, regions have an increasing number of outlier participants across progressive AD stages, with more pathological outliers (amyloid/tau) compared to atrophy outliers (MRI). The outlier frequency maps show spatial variability across modalities. The hippocampal region was the region with the highest MRI outlier percentage (47% of the CDR>= 1 group, 25% of the CDR = 0.5 group, 6% of the preclinical group and 3% of the cognitively unimpaired subjects). The highest percentage of amyloid outliers are present in the accumbens area region (95% of the CDR>= 1 group, 78% of the CDR = 0.5 group, 64% of the preclinical group) left putamen (3% of the cognitively unimpaired subjects). For tau, the amygdala regions showed the highest percentage of tau outliers (76% of the CDR>= 1 group, 57% of the CDR = 0.5 group, 28% of the preclinical group and 15% of cognitively unimpaired subjects). The outlier frequency maps of the Knight ADRC participants are presented in the Supplementary material (eFigure 5).

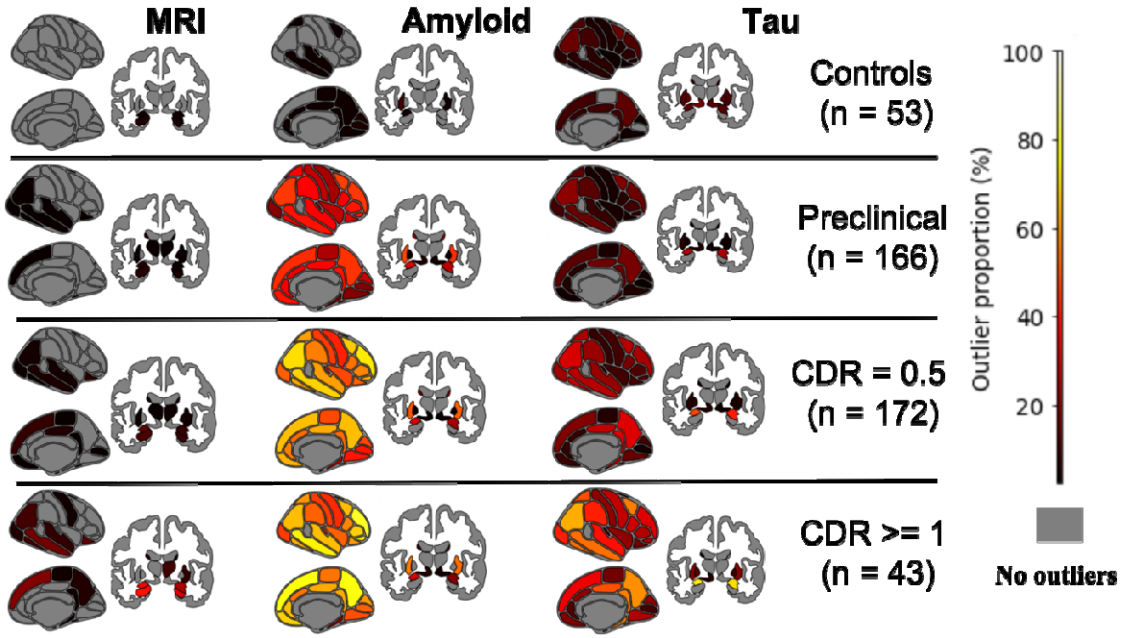

Figure 4: Regional brain atlas maps showing the percentage of outliers (FDR-corrected) within each participant group for the 3 modalities: MRI, amyloid and tau (from left to right). The numbers in

parentheses in each row indicate the number of participants within each group. The color bar represents the outlier proportion of each region from 0 to 100%. Gray represents that no participants have outlier deviations for that region.

Subject-level disease severity values are associated with cognition performance.

Linear regression adjusted by age and sex showed that there are significant associations between memory performance and disease severity values of ADNI participants calculated across all modalities ($\beta = -0.6$, $p = 2.5 \times 10^{-17}$), only MRI ($\beta = -0.04$, $p = 2.9 \times 10^{-7}$), only amyloid ($\beta = -0.56$, $p = 5.9 \times 10^{-7}$), and only tau ($\beta = -1.1$, $p = 1.3 \times 10^{-16}$). Similarly, executive function is also significantly associated with disease severity values for all modalities ($\beta = -0.4$, $p = 4.2 \times 10^{-13}$), only MRI ($\beta = -0.02$, $p = 8.7 \times 10^{-4}$), only amyloid ($\beta = -0.4$, $p = 1.8 \times 10^{-4}$), and only tau ($\beta = -0.8$, $p = 2.4 \times 10^{-13}$). The Pearson correlation coefficient values show that tau severity has a higher correlation with memory and executive scores than amyloid and MRI (Figure 5). For both ADNI-MEM and ADNI-EF, low scores indicate worse cognition performance. This is validated by the negative correlation between disease severity and cognition (or positive correlation between severity and worse cognition) for each modality (Figure 5).

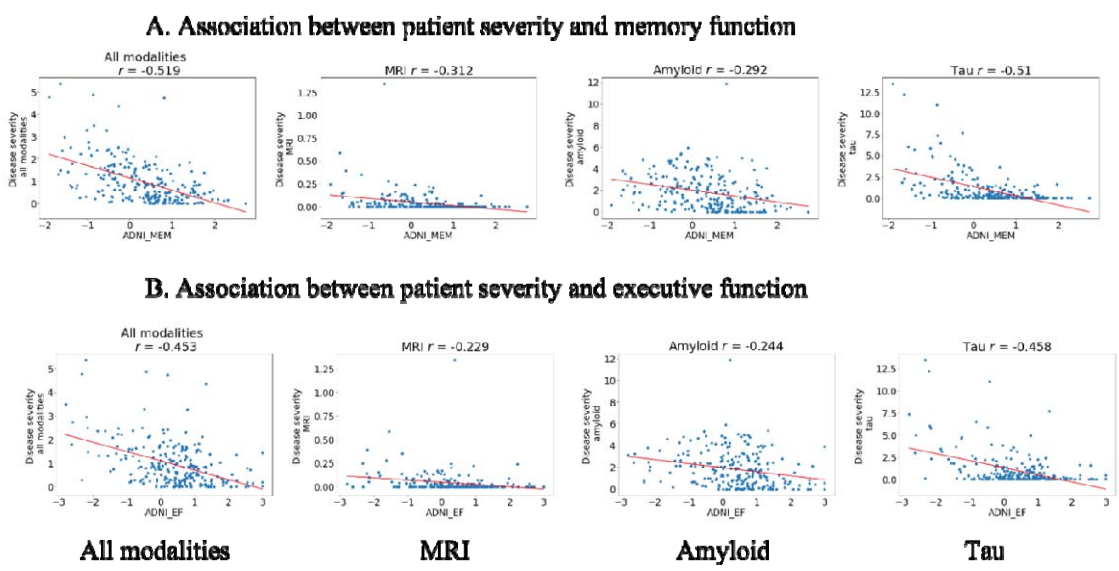

Figure 5: Association between the subject-level disease severity values and cognitive performance represented by composite memory score (A) and executive function (B) from the ADNI dataset. The x and y axes show the cognitive scores and the severity values respectively. The figures from left to right represent severity values across only modalities, only tau, only amyloid and only tau

respectively. r indicates the Pearson correlation coefficient value. Each point in the plot represents a subject and the red line denotes the linear regression fit of the points, adjusted by age and sex.

Higher disease severity values are associated with progression to advanced CDR stages

Survival analysis by the Cox proportional hazards model (adjusted by age and sex), indicated that disease severity values of subjects in the ADNI dataset are associated with the risk of converting from CDR < 1 to CDR >= 1 (hazard ratio 1.056, 95% CI 1.026–1.079, $p = 1.8 \times 10^{-11}$ (Figure 6). This is illustrated using a Kaplan-Meier plot, which shows that high disease severity ($3^{rd}/4^{th}$ quantile) can contribute to the risk of disease progression compared to low disease severity ($1^{st}/2^{nd}$ quantile).

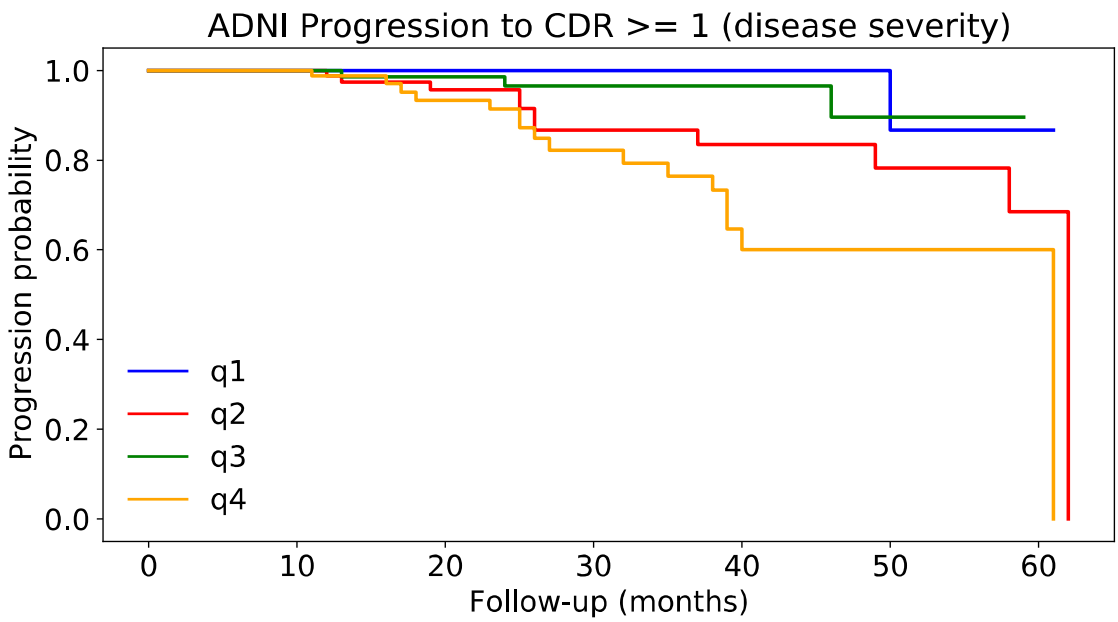

Figure 6: Kaplan-Meier plot of conversion from CDR < 1 to CDR >=1 for ADNI participants. The x-axis and the y-axis represent the follow-up period (in months) and the progression probability respectively. The 4 lines represent the 4 quantiles of subject-level disease severity across modalities, shown by blue, red, green and orange respectively. The filled color represents the 95% confidence intervals.

Discussion

In this study, our main goal was to (a) assess the spatial (regional) patterns of neuroanatomical and neuropathological variability in AD participants based on overlapping

or distinct pattern of outlier deviations and (b) quantify group differences in between-participant dissimilarity (patient-level heterogeneity) for each modality. Overall, the results of the present study show the extent of spatial variability in terms of outliers for each of the modalities. Patients in the advanced AD stages (a) have more morphological and pathological brain changes, (b) have more within-group subject-level heterogeneity and (c) have a higher proportion of outlier regional deviations than people with preclinical AD and cognitively unimpaired subjects. The severity values proposed in our study have been shown to be significantly associated with cognitive performance and potential markers to track disease progression.

Our findings both complement and offer additional information to the established understanding of AD. We observed high disease severity values in patients with advanced AD stages (Figure 1), consistent with the evidence of neurodegeneration (gray matter volume atrophy)[43] and neuropathological changes in the brain (accumulation of amyloid-tau proteins).[44] We observed more MRI outlier deviations (FDR-corrected) in temporal regions such as the hippocampus and amygdala (Figure 2). These are areas known to be sensitive to neurodegeneration in AD[45] and are associated with clinical symptoms in AD.[46] The observed variation in atrophy in the temporal lobe is also consistent with subtyping studies[11,47] and recent normative modelling studies[25,27]. Similarly, more tau deviations are present in the amygdala, entorhinal cortex, parahippocampus, fusiform, posterior cingulate, temporal, parietal, and frontal brain regions, areas known to have specific binding to ^{18}F AV1451 tau PET.[48] Amyloid outlier deviations are observed in the accumbens, precuneus, frontal and temporal regions, which are sensitive to ^{18}F AV45 amyloid PET accumulation.[49,50].

The severity scores proposed in our study are essentially Z-scores, estimating the extent to which AD subjects deviate from the healthy controls concerning gray matter volume (MRI atrophy) and pathological changes (amyloid and tau deposition). Previous studies have also estimated patient-level deviation metric by calculating either the average deviation or the total number of outlier deviations across all regions.[25,26,28] The study by Verdi et. al[25] proposed the total outlier count (TOC) metric which is the total number of outlier deviations across all regions. The severity values used in our study capture both the spatial extent of outliers (TOC) and the magnitude of regional outlier deviations, and quantify the spatial patterns of heterogeneity, both independently and aggregated across all modalities. Similar to

Verdi et. al,[25] we have shown that the severity values relate to cognition and disease progression. The disease severity index based on regional outlier estimates can be potentially used to track an individual's disease progression or treatment response in clinical trials.

Spatial heterogeneity in AD refers to the non-uniform distribution of pathological changes and brain abnormalities across different brain regions. For example, if atrophy pattern is fully homogenous, it is consistent across individuals or brain regions, indicating that most AD subjects are expected to have outliers in the same regions where MRI atrophy is observed. On the other hand, a heterogeneous pattern does not fully overlap between AD subjects, indicating that different individuals may exhibit outlier patterns in different brain regions for these markers. Looking beyond the group-average modality-specific regional differences, it was observed that the highest proportion of outliers in a single region was 54%, 75% and 94% for MRI, tau and amyloid respectively (Figure 4). This highlights the fact that amyloid is more homogenous in spatial patterns of outliers. However, MRI and tau are more heterogenous as individual spatial outlier patterns only partially overlap between AD subjects; if the outlier pattern is homogenous for a region (as assumed within group averages), 100% of subjects are expected to have outliers in that region. The spatial heterogeneity of MRI atrophy was also observed in the study by Verdi et. al where highest proportion of cortical thickness outliers in a single region was less than 50% in the AD group.

It can be observed from the results that amyloid PET and tau PET have more disease severity and outlier deviations compared to MRI (Figure 1,2,4). Pathology accumulation (amyloid first, then tau) are believed to occur early in the course of AD, even before clinical symptoms become apparent. In contrast, structural MRI volume ROI measures may show significant changes only at later stages when neurodegeneration and brain atrophy have already occurred. Moreover, amyloid and tau SUVR measures can detect small variations in pathological levels even before structural changes are visible on MRI. In contrast, MRI volume ROI measures may capture gross structural changes, such as significant brain atrophy, but may be less sensitive to early, subtle changes associated with AD pathology.

In this study, we cross-sectional imaging data for our normative modeling framework, providing a snapshot of the disease at a specific time. Due to our constraint that the MRI, amyloid and tau dates were within 1 year of one another, it was difficult to obtain significant number of multimodal follow-up visits. However, heterogeneity in AD has been

demonstrated to vary over time.[51] In future applications of multimodal normative modeling on AD data, it is important to incorporate serial neuroimaging data collected across multiple time points. This longitudinal approach will enable the characterization of patient-specific trajectories over time, improving treatment response at an individual patient level.

One interesting observation from our experimental results is that even cognitively unimpaired individuals exhibited outlier deviations in our study, indicating a certain level of within-group heterogeneity (as depicted in Figures 1 and 4). This is consistent with the findings of the study by Verdi et. al [25], which assumed “Cognitively Normal” people as the control cohort to measure heterogeneity in cortical thickness atrophy. This observation suggests that caution should be exercised when assuming homogeneity even within control groups in case-control studies. Statistical designs in basic research and clinical trials must take into account this inherent heterogeneity in brain structure to select a cleaner control cohort for more accurate and representative results.

Compared to subtyping studies, our normative modelling framework provides outlier maps of individual patient variability, which can be a better alternative to parse the heterogeneity of the AD cohort. An important scope for future work can be using the outlier deviations obtained as normative modelling output for clustering subjects into data-driven biological AD subtypes. The training of the normative approach does not rely on any specific labels, making it applicable to a wide range of clinical tasks including diagnosis, prognosis, treatment selection, and mechanistic inference for various brain disorders. Notably, there is no need for re-training or fine-tuning when applying the approach to different clinical tasks. Furthermore, since the approach involves anomaly detection, it can complement conventional discriminative models in identifying and addressing scenarios where supervised methods might fail catastrophically due to encountering test examples that are significantly different from the training set ("out-of-distribution" examples).

Conclusion

AD affects different subjects’ brains in different ways; this neurobiological heterogeneity aligns with the common observations of clinical heterogeneity. In this study, we provide a quantitative approach to estimate the variability in individual subjects' brain atrophy and neuropathological characteristics at the regional level, based on overlapping or distinct

patterns of outlier deviations. The disease severity maps based on neuroanatomical and neuropathological outliers were related to cognitive performance and can be used for predicting progression to advanced CDR stages. The subject-level outlier deviation maps derived from multimodal normative modelling can be a potential marker of AD state and evaluate the effectiveness of potential disease-modifying treatments tailored to the individual subject.

Acknowledgements

We would like to thank the staff of the Washington University Center for High Performance Computing who helped enable this work.

Funding

This work was supported by the National Institutes of Health (NIH) (R01-AG067103). Computations were performed using the facilities of the Washington University Center for High-Performance Computing, which were partially funded by NIH grant S10 OD025200. Additional support is provided by The McDonnell Center for Systems Neuroscience.

Data collection and sharing for this project was funded by the Alzheimer's Disease Neuroimaging Initiative (ADNI) (National Institutes of Health Grant U01 AG024904) and DOD ADNI (Department of Defense award number W81XWH-12-2-0012). ADNI is funded by the National Institute on Aging, the National Institute of Biomedical Imaging and Bioengineering, and through generous contributions from the following: AbbVie, Alzheimer’s Association; Alzheimer’s Drug Discovery Foundation; Araclon Biotech; BioClinica, Inc.; Biogen; Bristol-Myers Squibb Company; CereSpir, Inc.; Cogstate; Eisai Inc.; Elan Pharmaceuticals, Inc.; Eli Lilly and Company; EuroImmun; F. Hoffmann-La Roche Ltd and its affiliated company Genentech, Inc.; Fujirebio; GE Healthcare; IXICO Ltd.; Janssen Alzheimer Immunotherapy Research & Development, LLC.; Johnson & Johnson Pharmaceutical Research & Development LLC.; Lumosity; Lundbeck; Merck & Co., Inc.; Meso Scale Diagnostics, LLC.; NeuroRx Research; Neurotrack Technologies; Novartis Pharmaceuticals Corporation; Pfizer Inc.; Piramal Imaging; Servier; Takeda Pharmaceutical Company; and Transition Therapeutics. The Canadian Institutes of Health Research is providing funds to support ADNI clinical sites in Canada. Private sector contributions are

facilitated by the Foundation for the National Institutes of Health (www.fnih.org). The grantee organization is the Northern California Institute for Research and Education, and the study is coordinated by the Alzheimer's Therapeutic Research Institute at the University of Southern California. ADNI data are disseminated by the Laboratory for Neuro Imaging at the University of Southern California.

Data were provided (in part) by Knight Alzheimer Disease Research Center (ADRC), supported by grants P50-AG05681, P01- AG03991, and P01-AG26276 awarded to Dr Morris. AV-45 doses were provided by Avid Radiopharmaceuticals, a wholly-owned subsidiary of Eli Lilly.

Competing interests

Author AS has equity in TheraPanacea and has received personal compensation for serving as a grant reviewer for BrightFocus Foundation. The remaining authors have no conflicting interests to report.

Supplementary material

Supplementary material is available in a separate document

References

1. Kumar S, Oh I, Schindler S, Lai AM, Payne PR, Gupta A. Machine learning for modeling the progression of Alzheimer disease dementia using clinical data: a systematic literature review. JAMIA Open. Oxford University Press; 2021;4:ooab052.

2. Richards M, Brayne C. What do we mean by Alzheimer's disease? BMJ. British Medical Journal Publishing Group; 2010;341.

3. Jack CR, Knopman DS, Jagust WJ, et al. Hypothetical model of dynamic biomarkers of the Alzheimer's pathological cascade. Lancet Neurol. Elsevier; 2010;9:119–128.

4. Seeley WW. Mapping neurodegenerative disease onset and progression. Cold Spring Harb Perspect Biol. Cold Spring Harbor Lab; 2017;9:a023622.

5. Mehta RI, Schneider JA. What is 'Alzheimer's disease'? The neuropathological heterogeneity of clinically defined Alzheimer's dementia. Curr Opin Neurol. LWW; 2021;34:237–245.

6. Young PN, Estarellas M, Coomans E, et al. Imaging biomarkers in neurodegeneration: current and future practices. Alzheimers Res Ther. BioMed Central; 2020;12:1–17.

7. Habes M, Grothe MJ, Tunc B, McMillan C, Wolk DA, Davatzikos C. Disentangling heterogeneity in Alzheimer's disease and related dementias using data-driven methods. Biol Psychiatry. Elsevier; 2020;88:70–82.

8. Johnson KA, Fox NC, Sperling RA, Klunk WE. Brain imaging in Alzheimer disease. Cold Spring Harb Perspect Med. Cold Spring Harbor Laboratory Press; 2012;2:a006213.

9. Dubois B, Hampel H, Feldman HH, et al. Preclinical Alzheimer's disease: definition, natural history, and diagnostic criteria. Alzheimers Dement. Elsevier; 2016;12:292–323.

10. Lorenzi M, Simpson IJ, Mendelson AF, et al. Multimodal image analysis in Alzheimer's disease via statistical modelling of non-local intensity correlations. Sci Rep. Nature Publishing Group; 2016;6:1–8.

11. Dong A, Toledo JB, Honnorat N, et al. Heterogeneity of neuroanatomical patterns in prodromal Alzheimer's disease: links to cognition, progression and biomarkers. Brain. Oxford University Press; 2017;140:735–747.

12. Wen J, Varol E, Sotiras A, et al. Multi-scale semi-supervised clustering of brain images: Deriving disease subtypes. Med Image Anal. Elsevier; 2022;75:102304.

13. Ten Kate M, Dicks E, Visser PJ, et al. Atrophy subtypes in prodromal Alzheimer's disease are associated with cognitive decline. Brain. Oxford University Press; 2018;141:3443–3456.

14. Young AL, Marinescu RV, Oxtoby NP, et al. Uncovering the heterogeneity and temporal complexity of neurodegenerative diseases with Subtype and Stage Inference. Nat Commun. Nature Publishing Group UK London; 2018;9:4273.

15. Mohanty R, Mårtensson G, Poulakis K, et al. Comparison of subtyping methods for neuroimaging studies in Alzheimer's disease: a call for harmonization. Brain Commun. 2020;2:fcaa192.

16. Marquand AF, Wolfers T, Mennes M, Buitelaar J, Beckmann CF. Beyond lumping and splitting: a review of computational approaches for stratifying psychiatric disorders. Biol Psychiatry Cogn Neurosci Neuroimaging. Elsevier; 2016;1:433–447.

17. Graff-Radford J, Yong KX, Apostolova LG, et al. New insights into atypical Alzheimer's disease in the era of biomarkers. Lancet Neurol. Elsevier; 2021;20:222–234.

18. Marquand AF, Kia SM, Zabihi M, Wolfers T, Buitelaar JK, Beckmann CF. Conceptualizing mental disorders as deviations from normative functioning. Mol Psychiatry. Nature Publishing Group UK London; 2019;24:1415–1424.

19. Bethlehem RA, Seidlitz J, Romero-Garcia R, Trakoshis S, Dumas G, Lombardo MV. A normative modelling approach reveals age-atypical cortical thickness in a subgroup of males with autism spectrum disorder. Commun Biol. Nature Publishing Group UK London; 2020;3:486.

20. Huizinga W, Poot DH, Vernooij MW, et al. A spatio-temporal reference model of the aging brain. NeuroImage. Elsevier; 2018;169:11–22.

21. Kia SM, Marquand AF. Neural processes mixed-effect models for deep normative modeling of clinical neuroimaging data. Int Conf Med Imaging Deep Learn. PMLR; 2019. p. 297–314.

22. Marquand AF, Rezek I, Buitelaar J, Beckmann CF. Understanding heterogeneity in clinical cohorts using normative models: beyond case-control studies. Biol Psychiatry. Elsevier; 2016;80:552–561.

23. Ziegler G, Ridgway GR, Dahnke R, Gaser C, Initiative ADN. Individualized Gaussian process-based prediction and detection of local and global gray matter abnormalities in elderly subjects. Neuroimage. Elsevier; 2014;97:333–348.

24. Wolfers T, Doan NT, Kaufmann T, et al. Mapping the heterogeneous phenotype of schizophrenia and bipolar disorder using normative models. JAMA Psychiatry. American Medical Association; 2018;75:1146–1155.

25. Verdi S, Kia SM, Yong KX, et al. Revealing individual neuroanatomical heterogeneity in Alzheimer disease using neuroanatomical normative modeling. Neurology. AAN Enterprises; 2023;100:e2442–e2453.

26. Pinaya WH, Scarpazza C, Garcia-Dias R, et al. Using normative modelling to detect disease progression in mild cognitive impairment and Alzheimer's disease in a cross-sectional multi-cohort study. Sci Rep. Springer; 2021;11:1–13.

27. Pinaya WH, Mechelli A, Sato JR. Using deep autoencoders to identify abnormal brain structural patterns in neuropsychiatric disorders: A large-scale multi-sample study. Hum Brain Mapp. Wiley Online Library; 2019;40:944–954.

28. Kumar S, Payne PR, Sotiras A. Normative modeling using multimodal variational autoencoders to identify abnormal brain volume deviations in Alzheimer's disease. Med Imaging 2023 Comput-Aided Diagn. SPIE; 2023. p. 1246503.

29. Mueller SG, Weiner MW, Thal LJ, et al. Ways toward an early diagnosis in Alzheimer's disease: the Alzheimer's Disease Neuroimaging Initiative (ADNI). Alzheimers Dement. Elsevier; 2005;1:55–66.

30. Pomponio R, Erus G, Habes M, et al. Harmonization of large MRI datasets for the analysis of brain imaging patterns throughout the lifespan. NeuroImage. Elsevier; 2020;208:116450.

31. Fortin J-P, Cullen N, Sheline YI, et al. Harmonization of cortical thickness measurements across scanners and sites. Neuroimage. Elsevier; 2018;167:104–120.

32. Mueller SG, Weiner MW, Thal LJ, et al. The Alzheimer's disease neuroimaging initiative. Neuroimaging Clin. Elsevier; 2005;15:869–877.

33. Fischl B. FreeSurfer. Neuroimage. Elsevier; 2012;62:774–781.

34. Desikan RS, Ségonne F, Fischl B, et al. An automated labeling system for subdividing the human cerebral cortex on MRI scans into gyral based regions of interest. Neuroimage. Elsevier; 2006;31:968–980.

35. Fischl B, Salat DH, Busa E, et al. Whole brain segmentation: automated labeling of neuroanatomical structures in the human brain. Neuron. Elsevier; 2002;33:341–355.

36. Shaw LM, Vanderstichele H, Knapik-Czajka M, et al. Cerebrospinal fluid biomarker signature in Alzheimer's disease neuroimaging initiative subjects. Ann Neurol. Wiley Online Library; 2009;65:403–413.

37. Su Y, Flores S, Wang G, et al. Comparison of Pittsburgh compound B and florbetapir in cross-sectional and longitudinal studies. Alzheimers Dement Diagn Assess Dis Monit. Wiley Online Library; 2019;11:180–190.

38. Cao Y, Fleet DJ. Generalized product of experts for automatic and principled fusion of Gaussian process predictions. ArXiv Prepr ArXiv14107827. Epub 2014.

39. Wu M, Goodman N. Multimodal generative models for scalable weakly-supervised learning. Adv Neural Inf Process Syst. 2018;31.

40. Benjamini Y, Hochberg Y. Controlling the false discovery rate: a practical and powerful approach to multiple testing. J R Stat Soc Ser B Methodol. Wiley Online Library; 1995;57:289–300.

41. Crane PK, Carle A, Gibbons LE, et al. Development and assessment of a composite score for memory in the Alzheimer's Disease Neuroimaging Initiative (ADNI). Brain Imaging Behav. Springer; 2012;6:502–516.

42. Gibbons LE, Carle AC, Mackin RS, et al. A composite score for executive functioning, validated in Alzheimer's Disease Neuroimaging Initiative (ADNI) participants with baseline mild cognitive impairment. Brain Imaging Behav. Springer; 2012;6:517–527.

43. Jack CR, Shiung MM, Gunter JL, et al. Comparison of different MRI brain atrophy rate measures with clinical disease progression in AD. Neurology. AAN Enterprises; 2004;62:591–600.

44. Morishima-Kawashima M, Ihara Y. Alzheimer's disease: β-Amyloid protein and tau. J Neurosci Res. Wiley Online Library; 2002;70:392–401.

45. Popuri K, Ma D, Wang L, Beg MF. Using machine learning to quantify structural MRI neurodegeneration patterns of Alzheimer's disease into dementia score: Independent validation on 8,834 images from ADNI, AIBL, OASIS, and MIRIAD databases. Hum Brain Mapp. Wiley Online Library; 2020;41:4127–4147.

46. Leech R, Sharp DJ. The role of the posterior cingulate cortex in cognition and disease. Brain. Oxford University Press; 2014;137:12–32.

47. Noh Y. Anatomical heterogeneity of Alzheimer. Epub 2014.

48. Zhao Q, Liu M, Ha L, Zhou Y, Initiative ADN. Quantitative 18F-AV1451 brain tau PET imaging in cognitively normal older adults, mild cognitive impairment, and Alzheimer's disease patients. Front Neurol. Frontiers Media SA; 2019;10:486.

49. Wong DF, Rosenberg PB, Zhou Y, et al. In vivo imaging of amyloid deposition in Alzheimer disease using the radioligand 18F-AV-45 (flobetapir F 18). J Nucl Med. Soc Nuclear Med; 2010;51:913–920.

50. Levitis E, Vogel JW, Funck T, et al. Differentiating amyloid beta spread in autosomal dominant and sporadic Alzheimer's disease. Brain Commun. Oxford University Press; 2022;4:fcac085.

51. Ferreira D, Verhagen C, Hernández-Cabrera JA, et al. Distinct subtypes of Alzheimer's disease based on patterns of brain atrophy: longitudinal trajectories and clinical applications. Sci Rep. Nature Publishing Group UK London; 2017;7:46263.